Journal of Geosciences, 59 (2014), 99–114 DOI: 10.3190/jgeosci.163

Review

Oxidation–hydration weathering of uraninite: the current state-of-knowledge

Jakub PLÁŠIL

Institute of Physics, Academy of Sciences of the Czech Republic v.v.i, Na Slovance 2, 182 21, Prague 8, Czech Republic; plasil@fzu.cz

Oxidation–hydration weathering of uraninite, the most common U-bearing mineral in nature, comprises various physical and chemical processes that lead to the destruction of the fluorite-type structure of uraninite where U is present as tetravalent. This results in replacement of uraninite by weathering products containing U in hexavalent form, i.e. as uranyl ion, UO_2^{2+}. The final assemblage of the weathering products, uranyl minerals, and their compositions depend on the various factors, namely the composition of the primary minerals and percolating oxidizing fluids that cause the alteration. The knowledge of such processes and stabilities of the uranium minerals is of the great interest namely due to demand for U as the energy source. During the past decade there has been substantial progress in understanding the mineralogy, crystallography and thermodynamics of uranyl minerals and thus a substantially improved understanding of the weathering processes themselves. This review aims to summarize the state-of-art of the current knowledge on uranium-related topics as well and identify some of the important questions that remain unanswered.

The following text is dedicated to Jiří Čejka on occasion of his 85th birthday anniversary. Jiří greatly contributed not only to the spectroscopy and mineralogy of uranyl minerals, but also to the questions pertaining their origin and stability. Many important issues were addressed, even if briefly, in the pioneering book "Secondary Uranium Minerals" by Čejka and Urbanec (1990) which has served, for a long-time, as a guide for beginning uranium mineralogists.

Keywords: weathering of uraninite, paragenetic sequence, bond-valence theory, uranyl–oxide minerals, radiogenic lead, thermodynamics
Received: 10 December 2013; accepted: 16 March 2014; handling editor: J. Sejkora

1. Introduction

Uraninite, ideally cubic ($Fm\overline{3}m$) UO_2, however, never occurs in Nature as stoichiometrically pure U^{4+} oxide, but rather as UO_{2+x} (where x = 0–0.25) (Janeczek and Ewing 1992). Most commonly is uraninite found in the colomorph form known as "*pitchblende*" (Fig. 1a), which undergoes rapid alteration in a humid, oxidizing environment. The corrosion process is described as "oxidation–hydration weathering". This process leads to the decomposition of the uraninite structure, primarily *via* the oxidation of U^{4+} to U^{6+}, which is, in general, incompatible with the uraninite structure. Moreover it includes also leaching or replacement of uraninite by the younger minerals – supergene weathering products, usually containing U^{6+} in their crystal structures. The leaching of uraninite leads to the release of U^{6+}, as the uranyl ion $(UO_2)^{2+}$, into the solution, where it exists as aquatic anionic complexes (depending on the pH of the solution and concentration of dissolved anions). In weakly acidic to weakly alkaline solutions (matching properties of most groundwaters) the uranyl carbonate complexes are thermodynamically favored when CO_2 is a dominant aqueous species. The most abundant aqueous species are then uranyl monocarbonate, $[(UO_2)(CO_3)]^0$, uranyl dicarbonate, $[(UO_2)(CO_3)_2]^{2-}$ and uranyl tricarbonate, $[(UO_2)(CO_3)_3]^{4-}$, complexes at pK values of 5.5, 7 and 9, respectively (Langmuir 1978). In the form of aquatic anionic complexes, the U^{6+} ion is very mobile and can migrate for a long distance. Therefore many uranyl minerals may be found without any obvious spatial relation to the primary ore (Fig. 1b). The *in-situ* alteration products replacing directly the uraninite aggregates are known mostly as "*gummites*" (Fig. 1c). This obsolete, however still useful name, is used for massive, often layered and microcrystalline, mixtures of the diverse compositions (described for the first time by Frondel 1956) replacing uraninite. The proportion of the mineral components in "gummites" depends on a variety of factors e.g., the rate of groundwater percolation and its chemical composition, the age of uraninite and its chemical composition (e.g., Pb content). Studying the mechanisms and products of the oxidation–hydration weathering of uraninite is important for better understanding of both the genesis of uranium deposits (particularly important for mineral exploration) and dissolution, transport and retardation/immobilization of environmentally harmful elements such as uranium, other radionuclides, Se and Pb. During the last decades an impressive step forward has been taken in the many new studies that have added to the knowledge of the crystal chemistry of uranium, the thermodynamics of the uranyl minerals, and the important physical processes connected to the weathering (dissolution, precipitation, etc.). This paper is not meant to be an exhaustive review of all of

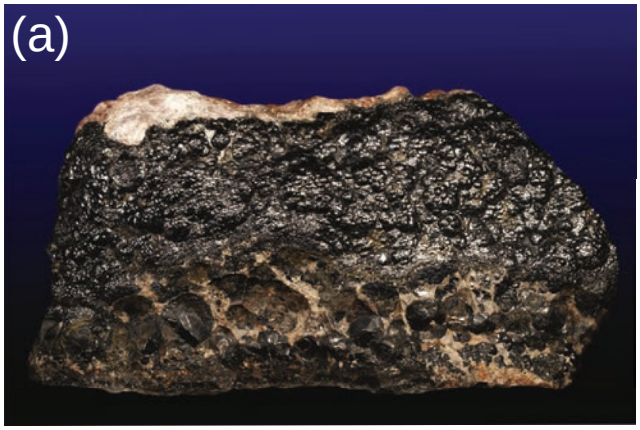

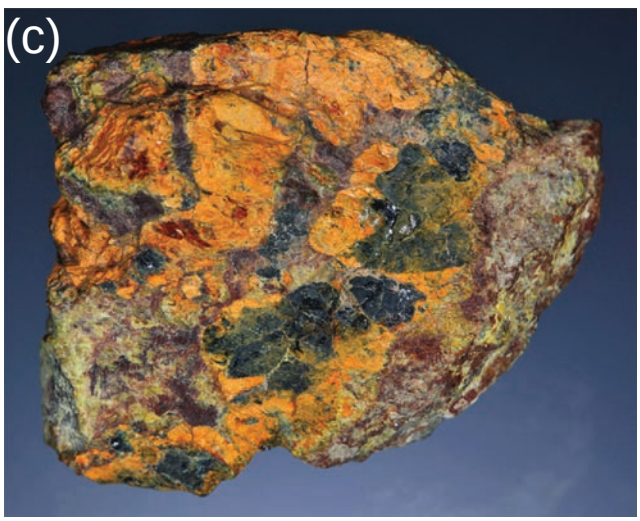

Fig. 1a – Uraninite in the form of "pitchblende" in calcite gangue. The pit #15, Příbram uranium deposit. The width of the photograph (field-of-view, FOV) 15 cm, photo P. Škácha. **b –** Efflorescence of schröckingerite (showing greenish fluorescence in the UV lamp light) on the wall of the mining adit without any significant primary uranium mineralization. Svornost mine, Jáchymov; photo P. Škácha. **c –** "Gummite" – residual uraninite (blackish) being replaced by orange masuyite. Dump of the Rovnost mine, Jáchymov. The width of the sample is 4 cm. Photo P. Škácha.

the mentioned issues, but it is rather a brief summary of the current knowledge on uranium-related topics (mainly from the mineralogical point of the view). Moreover, it aims to identify several still unclosed gaps in the knowledge of uranium minerals.

1.1. Uraninite and spent nuclear fuel

The moving power for the studies undertaken namely in 1990s was the rising energy consumption and related demand to use uranium as an energy source. This has been connected with an increased pressure for the disposal of spent nuclear fuel (SNF), which consists of irradiated UO_2, in underground geologic repositories (Wronkiewicz et al. 1992; Ewing 1993; Janeczek et al. 1996). Long-term tests of the stability and durability of SNF exposed to the weathering (air, mineralized solutions and/or increased temperature), as may happen in underground repositories when engineered barriers fail, have been undertaken (Wronkiewicz et al. 1992, 1996). Numerous studies on natural uraninite as an analogue for SNF (Janeczek et al. 1996) were undertaken with the particular interest both in physico-chemical processes that occur during the alteration (e.g., Finch and Ewing 1992; Isobe et al. 1992; Pearcy et al. 1994; Finch et al. 1996; Murakami et al. 1997; Schindler and Hawthorne 2004; Schindler and Putnis 2004; Schindler et al. 2004a, b, c; Deditius et al. 2007a, b, 2008; Schindler et al. 2011; Forbes et al. 2011) and in the formation of supergene phases as the concentrators of the elements of the interest – uranium and possible fission products (such as Pu, Sr, Np) (Burns et al. 1997a, b; Burns 1999a; Burns and Hill 2000; Cahill and Burns 2000; Li and Burns 2001; Burns and Li 2002; Burns et al. 2004; Klingensmith and Burns 2007; Klingensmith et al. 2007). The long-term tests (Wronkiewicz et al. 1992, 1996) showed that the alteration mechanisms for nuclear fuel and uraninite lead to the same weathering products.

2. Uranyl minerals – products of weathered uraninite

2.1. Mineralogy and crystallography

During the last decades there has been a substantial increase in the knowledge of the mineralogy and crystal

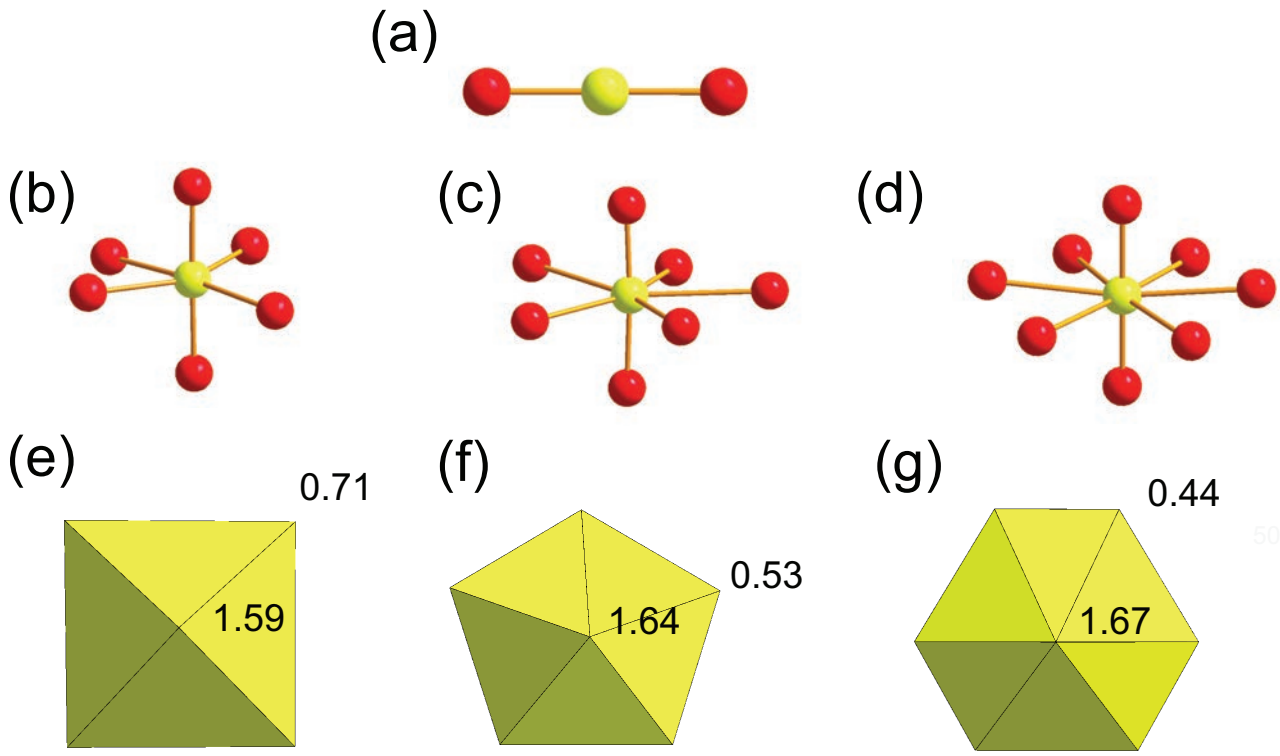

Fig. 2 Ball-and-stick representation of the uranyl ion, UO_2^{2+} (**a**), tetragonal (**b**), pentagonal (**c**) and hexagonal (**d**) bipyramids, as well as their corresponding polyhedral representations (**e–g**) with the bond-valence sums (in valence units) incident upon each vertex owing to the U^{6+}–O bond within the polyhedra (values from Burns et al. 1997a).

chemistry of uranium, especially of phases containing U^{6+} (Burns et al. 1996, 1997a; Burns 1999b, 2005; Krivovichev and Plášil 2013). This fact was possible due to the increasing capabilities of the analytical techniques, namely in the field of X-ray diffraction and CCD imaging techniques (Burns 1998a) used as a tool for crystal structure determination.

The mineralogy of hexavalent uranium is extremely diverse due to the specific electronic properties of U in such a high-valence state, which leads to the highly anisotropic coordination polyhedra around the U^{6+} cation. The U^{6+} exists as the uranyl ion UO_2^{2+}, where the two O atoms (O_{Ur} atoms) are strongly bonded (a triple-bond) in a nearly-linear, dumbbell-like (Fig. 2a), geometry to a central U atom at the distances ranging most commonly from ~1.78 to ~1.81 Å (Burns et al. 1997a), depending on the type of the coordination polyhedra. The physicochemical properties of the uranyl ion are unique, and thus it cannot be easily substituted by any other high-valence cation. To satisfy the bond-valence requirements, the uranyl ion needs to be coordinated to more ligands, usually O atoms (O_{eq}). These additional ligands are arranged at relatively long distances from the central U^{6+} at the equatorial vertices of the uranyl tetragonal (4 equatorial ligands at the distance ~2.30 Å) (Fig. 2b), pentagonal (5 ligands, ~2.37 Å) (Fig. 2c) or hexagonal (6 ligands, ~2.46 Å) (Fig. 2d) bipyramids, with O_{Ur} atoms at the vertices (Burns et al. 1997a; Burns 2005). The ligand atoms are usually undersaturated in terms of their bond-valence requirements (Fig. 2e–g) and tend to polymerize, thus forming clusters, chains, sheets or three-dimensional frameworks with incorporated additional cations, most commonly coordinated in tetrahedral anionic groups (e.g. SO_4^{2-}, PO_4^{3-}, AsO_4^{3-}, SiO_4^{4-}). In order to simplify and classify the crystal structures of uranyl minerals, the structural hierarchy of the structures was developed based on the topologies of the basic structure units – uranyl anion topologies (Burns et al. 1996; Burns 1999b, 2005) following the general idea of Hawthorne (1983, 1994) and in accord with the bond-valence theory (Brown 1981, 2002, 2009). The topologies of the structural units (Fig. 3a) of uranyl minerals and compounds, which are the "consolidated" parts of the structures that contain cations of higher valence and have anionic character, are represented by corresponding graphs. The anion topology can be derived using the following rules (Burns 2007): (1) only O_{eq} atoms are considered that are bonded to two or more cations within the layer, (2) the O_{eq} atoms that are separated by less than 3.5 Å are connected by lines (Fig. 3b), (3) all atoms are removed from consideration and the resulting tiling is projected onto a 2-D plane (Fig. 3c). Burns (2005) presented 368 inorganic crystal structures containing U^{6+}, of which 89 were minerals. Based on this analysis, eight were based upon isolated

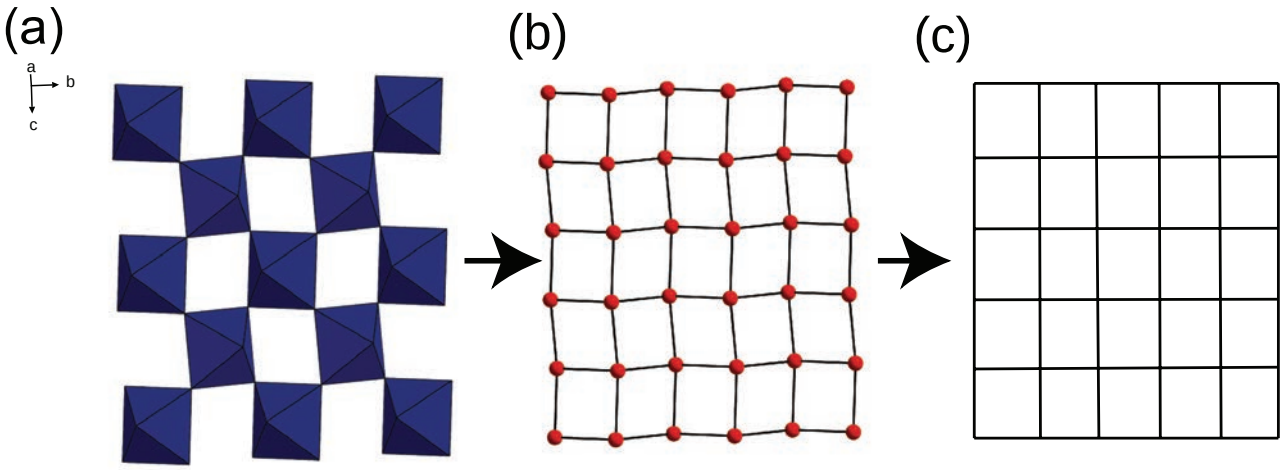

Fig. 3 The sheet of polyhedra in the structure of γ-$(UO_2)(OH)_2$ (**a**), square-grid consisting of equatorial O atoms (**b**) and the idealized graph of its (autunite) topology (**c**).

polyhedra, 43 upon finite clusters, 57 upon chains, 204(!) upon sheets, and 56 upon frameworks of polyhedra. The most recent overview on the mineralogy and crystallography of uranium has been given by Krivovichev and Plášil (2013). Many new uranium minerals with a diverse chemical composition and fascinating structures have been described in the past few years (e.g., Sejkora and Čejka 2007; Mills et al. 2008; Walenta et al. 2009; Meisser et al. 2010; Kampf et al. 2010; Plášil et al. 2010a; Brugger et al. 2011; Plášil et al. 2011a, b; Pekov et al. 2012a, b; Plášil et al. 2012a, b, c; Walenta and Theye 2012; Kampf et al. 2013; Pekov et al. 2013; Plášil et al. 2013a, b, c). Nowadays, more than 260 minerals (!) are known to contain U in their crystal structures (not all of the U-structures are known).

2.2. *The role of uranyl-oxide–hydroxy–hydrates in the evolution of uraninite (SNF)-weathering paragenetic sequences and the role of radiogenic Pb*

Uranyl-oxide–hydroxy–hydrate minerals play a key role in alteration of uraninite as the very initial alteration phases in the weathering paragenetic sequences (Finch and Ewing 1992; Finch and Murakami 1999; Krivovichev and Plášil 2013). There are numerous research papers devoted to the issue of the uranyl–oxide minerals and their significance during the uraninite weathering (e.g., Finch and Ewing 1992; Finch et al. 1996; Burns 1997; Burns et al. 1997b; Burns 1998b, c; Finch et al. 1998; Schindler and Hawthorne 2004; Brugger et al. 2004; Hazen et al. 2009; Brugger et al. 2011). Several different alteration pathways are generally accepted. The very beginning phase of the alteration is common for distinct pathways: uraninite is altered first to the metallic-cation-free mineral, such as ianthinite, $[U^{4+}(UO_2)_4O_6(OH)_4(H_2O)_4](H_2O)_5$ (Burns et al. 1997c) and further to schoepite, $[(UO_2)_8O_2(OH)_{12}](H_2O)_{12}$ (Finch et al. 1996) (Fig. 4). Schoepite and the closely-related phases, such as metaschoepite, $(UO_2)(OH)$ (Weller et al. 2000) and paulscherrerite (Brugger et al. 2011), represent a quite complex suite of minerals related by the dehydration processes (Finch et al. 1998). During the subsequent alteration, a complex suite of uranyl-oxide–hydroxy–hydrate minerals is developed. The overview of the known oxide–hydroxy–hydrate minerals is given in Tab. 1, along with their important crystal-chemical features. A two-stage weathering process was identified by Finch and Ewing (1992):

a) When the mineral system contains radiogenic Pb (its source being the "old uraninite"), a suite of Pb-containing uranyl–oxide minerals evolves during the alteration that is characterized by an increasing molar ratio of Pb^{2+}/H_2O as the function of the progressively

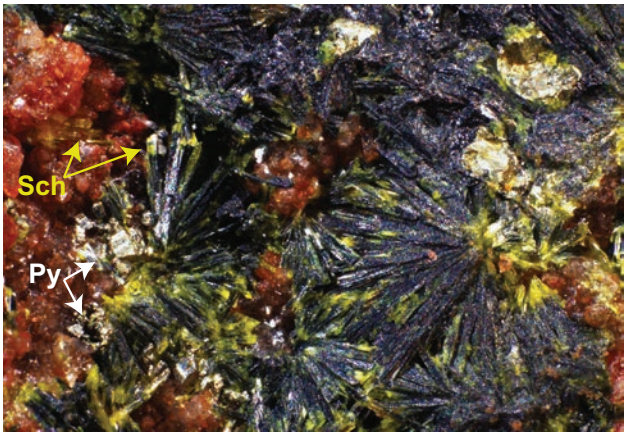

Fig. 4 Ianthinite (violet blackish) partly altered to schoepite (Sch; yellow) growing on pyrite (Py) grains in the barite gangue. Menzenschwand uranium deposit, Schwarzwald (Germany). FOV 3.4 mm, photo P. Škácha.

Tab. 1 Overview of the known uranyl-oxide–hydroxy–hydrate minerals or mineral-related synthetic materials with details on the stereochemical properties of their structural units

Mineral	Formula	Structural unit	CDA [*vu*]	Reference
schoepite	$[(UO_2)_8O_2(OH)_{12}](H_2O)_{12}$	$[(UO_2)_8O_2(OH)_{12}]^0$	0.08	Finch et al. (1996)
metaschoepite (synth.)	$[(UO_2)_4O(OH)_6](H_2O)_5$	$[(UO_2)_4O(OH)_6]^0$	0.08	Weller et al. (2000)
paulscherrerite	$UO_2(OH)_2$	$[(UO_2)(OH)_2]^0$	0.10	Brugger et al. (2011)
Na-metaschoepite (synth.)	$Na[(UO_2)_4O_2(OH)_5](H_2O)_5$	$[(UO_2)_4O_2(OH)_5]^{1-}$	0.13	Klingensmith et al. (2007)
heisenbergite	$(UO_2)(OH)_2(H_2O)$	$[(UO_2)(OH)_2]^0$	0.16	Walenta and Theye (2012)
becquerelite	$^{[7]}Ca(H_2O)_4[(UO_2)_3O_2(OH)_3]_2(H_2O)_4$	$[(UO_2)_3O_2(OH)_3]_2^{1-}$	0.145	Burns and Li (2002)
compreignacite	$^{[7]}K_2(H_2O)_3[(UO_2)_3O_2(OH)_3]_2(H_2O)_4$	$[(UO_2)_3O_2(OH)_3]_2^{1-}$	0.145	Burns (1998c)
billietite	$^{[10]}Ba(H_2O)_4[(UO_2)_3O_2(OH)_3]_2(H_2O)_3$	$[(UO_2)_3O_2(OH)_3]_2^{1-}$	0.145	Finch et al. (2006)
rameauite	$K_2Ca[(UO_2)_6O_4(OH)_6](H_2O)_6$	$[(UO_2)_3O_2(OH)_3]_2^{1-}$	0.145	Cesbron et al. (1972)
vandendriesscheite	$^{[9]}Pb_1{}^{[8]}Pb_{0.57}(H_2O)_5[(UO_2)_{10}O_6(OH)_{11}](H_2O)_6$	$[(UO_2)_{10}O_6(OH)_{11}]^{3-}$	0.14	Burns (1997)
fourmarierite	$^{[9]}Pb(H_2O)_2[(UO_2)_4O_3(OH)_4](H_2O)_2$	$[(UO_2)_4O_3(OH)_4]^{2-}$	0.19	Li and Burns (2000b)
agrinierite	$^{[8]}K_2{}^{[9]}(Ca,Sr)(H_2O)_5[(UO_2)_3O_3(OH)_2]_2$	$[(UO_2)_3O_3(OH)_2]^{2-}$	0.22	Cahill and Burns (2000)
richetite	$^{[6]}M_x{}^{[8.4]}Pb_{8.57}(H_2O)_{31}[(UO_2)_{18}O_{18}(OH)_{12}](H_2O)_{10}$	$[(UO_2)_3O_3(OH)_2]^{2-}$	0.22	Burns (1998b)
masuyite	$^{[10]}Pb(H_2O)_3[(UO_2)_3O_3(OH)_2]$	$[(UO_2)_3O_3(OH)_2]^{2-}$	0.22	Burns and Hanchar (1999)
protasite	$^{[10]}Ba_2(H_2O)_3[(UO_2)_3O_3(OH)_2]$	$[(UO_2)_3O_3(OH)_2]^{2-}$	0.22	Pagoaga et al. (1987)
curite	$^{[9]}Pb_3(H_2O)_2[(UO_2)_8O_8(OH)_6]$	$[(UO_2)_8O_8(OH)_6]^{6-}$	0.24	Li and Burns (2000a)
sayrite	$^{[9]}Pb_2(H_2O)_4[(UO_2)_5O_6(OH)_2]$	$[(UO_2)_5O_6(OH)_2]^{4-}$	0.24	Piret et al. (1983)
wölsendorfite	$^{[8.15]}(Pb_{6.2}Ba_{0.4})(H_2O)_{10}[(UO_2)_{14}O_{19}(OH)_4](H_2O)_2$	$[(UO_2)_{14}O_{19}(OH)_4]^{14-}$	0.29	Burns (1999c)
spriggite	$^{[8.4]}Pb_3[(UO_2)_6O_8(OH)_2](H_2O)_3$	$[(UO_2)_6O_8(OH)_2]^{6-}$	0.29	Brugger et al. (2004)

CDA – Charge Deficiency per Anion; calculated as the effective charge of the structural unit divided by the number of anions in the structural unit. The effective charge is the formal charge plus the charge contributed by the (H)-bonds in the structural unit = $n \times 0.2$.

increasing degree of alteration (with increasing time). Such a pathway is represented by the following paragenetic sequence: schoepite → vandendriesscheite → fourmarierite → masuyite → sayrite → curite → wölsendorfite → richetite → spriggite.

b) The system that does not contain radiogenic Pb (derived from the "young uraninite") is again characterized by the increasing molar ratio of *Me* (a metal cation) to H_2O with increasing degree of alteration. It is represented by the paragenetic sequence: schoepite → becquerelite (Ca^{2+}), billietite (Ba^{2+}), compreignacite (K^+) → agriniérite (Sr^{2+}) and protasite (Ba^{2+}) → clarkeite (Na^+).

There is a relation between the molecular proportion of water and content of metal cations in the uranyl–oxide minerals (Fig. 5). This was first documented by Finch and Ewing (1992), who showed that the changing ratio corresponds closely to the degree of alteration. The youngest alteration phases (the first formed from uraninite), such as schoepite, contain large amounts of H_2O and a little or no metal cations. With continuing alteration, the ratio between H_2O and *Me* decreases. Schindler and Hawthorne (2001) studied the paragenetic relations of borates examining the stereochemical properties of their structures (so called "the bond-valence approach"). They showed that there is a reasonable relation between the structural configuration of the hydrated oxysalts and the properties of the solution (pH and activity of dissolved elements) from which they precipitate. The measure related to the crystal structure they introduced is called the "*Charge Deficiency per Anion*" (CDA) and is given in *valence units*. The CDA is defined as the average bond-valence per O atom contributed by the interstitial species and adjacent structural units. This value correlates strongly with the average O-coordination number of the structural unit (which correlates extensively with the Lewis basicity of the structural unit), and hence it plays a crucial role in the predictive power of the crystal-chemical properties of these phases. For borate minerals, Schindler et al. (2001) documented that the borate structural units with the lower CDA values crystallize from the solution of the lower pH than the species with high CDA values. Using the same approach, Schindler and Hawthorne (2004) examined the uranyl-oxide–hydroxy–hydrates. They concluded that the restricted range in Lewis basicity, characterizing the structural units of uranyl-oxide–hydroxy–hydrates, is reflected by their narrow stability field. Further they provided *a priori* deduction of the relative stability fields of the uranyl-oxide–hydroxy–hydrates with respect to changing pH and composition (contents of metal cations) of the solution. Along with the increasing pH, there is a change in topologies of the structural units of uranyl-oxide–hydroxy–hydrates from the lower degree of polymerization (in schoepite) to higher degree of polymerization, i.e. topologies containing pentagonal and hexagonal bipyramids and fewer unoccupied triangles. The CDA values for known uranyl-oxide–hydroxy–hydrate minerals are given in Tab. 1. The dependence of CDA on the molar proportion of H_2O in these minerals (as the function of alteration degree) is illustrated in Fig. 5. Krivovichev and Plášil (2013) discussed the paragenetic scheme presented originally by Belova (1975, 2000) (see Fig. 6). This

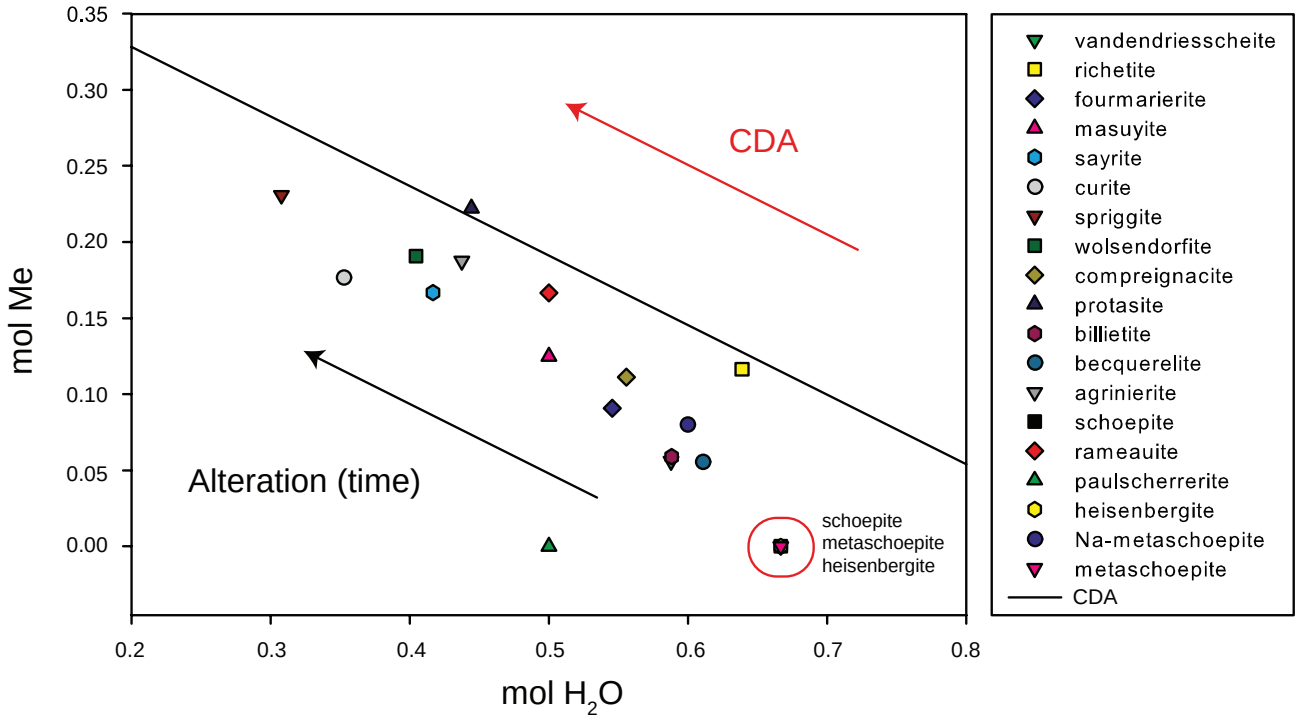

Fig. 5 Composition of uranyl-oxide–hydroxy–hydrate minerals as a function of molecular proportions of H_2O and *Me* (*Me* = metal cations). The solid black line represents regression trend (R^2 = 0.61) between molecular proportion of H_2O and the Charge-Deficiency per Anion (CDA) value (in valence units). The symbols for CDA are omitted for clarity. The scale of the y axis is the same for both datasets.

scheme represents another perspective on this complex system that leads to new ideas, summarized below.

1. During the initial stage, the alteration of primary uranium minerals takes place before the oxidation of sulfides at neutral or alkaline conditions caused by the presence of vein carbonates and alkali elements. This stage is dominated by the presence of uranyl oxide minerals (usually forming *gummite*) and corresponds to the early stages described by Finch and Ewing (1992). Uranyl carbonates are leached out due to the undersaturated percolating water (e.g. with low p_{CO2}), and U^{6+} can be released into the solution in the form of uranyl–carbonate complexes. This leads to the precipitation of uranyl–carbonate minerals, such as metal-free carbonates as rutherfordine, $(UO_2)(CO_3)$ (Fig. 7a) or containing monovalent or divalent metal cations as grimselite, $K_3Na[(UO_2)(CO_3)_3](H_2O)$ (Fig. 7b) or bayleyite, $Mg_2[(UO_2)(CO_3)_3](H_2O)_{18}$ (Fig. 7c), respectively. Noteworthy, uranyl carbonates can form a part of the "gummites". This was documented for example in case of the Pb^{2+}-containing uranyl carbonate widenmannite (Plášil et al. 2010b) or monocarbonate rutherfordine (Plášil et al. 2006). The occurrence of the unique, U^{5+}-bearing carbonate wyartite, $CaU^{5+}(UO_2)_2(CO_3)O_4(OH)(H_2O)_7$ (Burns and Finch 1999) (Fig. 7d) is also interesting, as is its position in the paragenetic scheme of the early alteration products after uraninite weathering. In the CO_2–UO_2^{2+}-bearing solutions after the dissolution of gangue carbonates, the UO_2^{2+} ion can be transported in the form of the aqua–carbonate complexes over long distances (Langmuir 1978). From such solutions in contact with the SO_4^{2-}-containing waters (derived from dissolved oxidized sulfides), minerals like schröckingerite, $NaCa_3[(UO_2)(CO_3)_3](SO_4)F(H_2O)_{10}$ (Mereiter 1986) can precipitate. Schröckingerite is one of the most widespread secondary uranyl minerals occurring in Nature; however, it is usually rather inconspicuous, forming most commonly efflorescence on the walls of the mining adits (Fig. 1b) (see also e.g., Klomínský et al. 2013). In the end of this stage uranyl silicate minerals may occur due to the increase in the Si^{4+} activity mainly released from the surrounding rocks due to proceeding alteration.
2. At the second stage, simultaneous massive alteration of uranium and sulfide minerals takes place. This stage begins with the oxidative weathering of basic sulfides (pyrite, marcasite, chalcopyrite, pyrrhotite and arsenopyrite), when the vein carbonates have been already leached out and can no longer buffer the solution composition. This results in the formation of the free sulfuric acid, as well as other acids, leading to acidic conditions. This results in the formation of uranyl sulfate minerals that may occur as minor alteration phases during the post-mining processes, known as the Acid-Mine Drainage (AMD) (e.g., Brugger et al. 2003) (Fig. 7e).

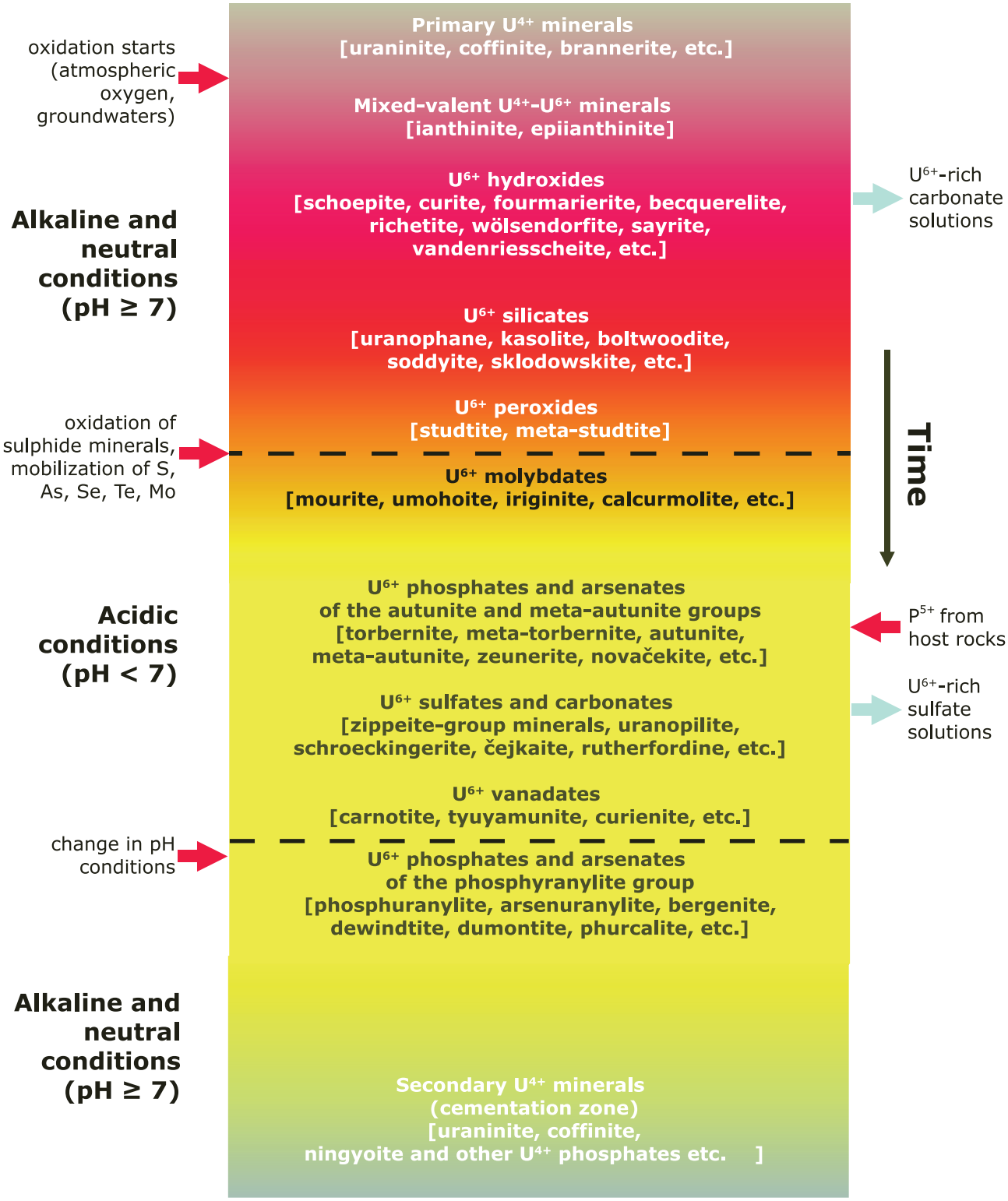

Fig. 6 Schematic representation of the paragenetic sequence of U minerals in oxidation zones of U mineral deposits (after Krivovichev and Plášil 2013).

3. The third stage takes place initially under the weakly acidic conditions and is represented by the occurrence of uranyl phosphates (P^{5+} from the host-rocks), such as torbernite, $Cu[(UO_2)(PO_4)]_2(H_2O)_{12}$, and arsenates ($As^{5+}$ from the residue after dissolved arsenides), as zeunerite, $Cu[(UO_2)(AsO_4)]_2(H_2O)_{12}$.

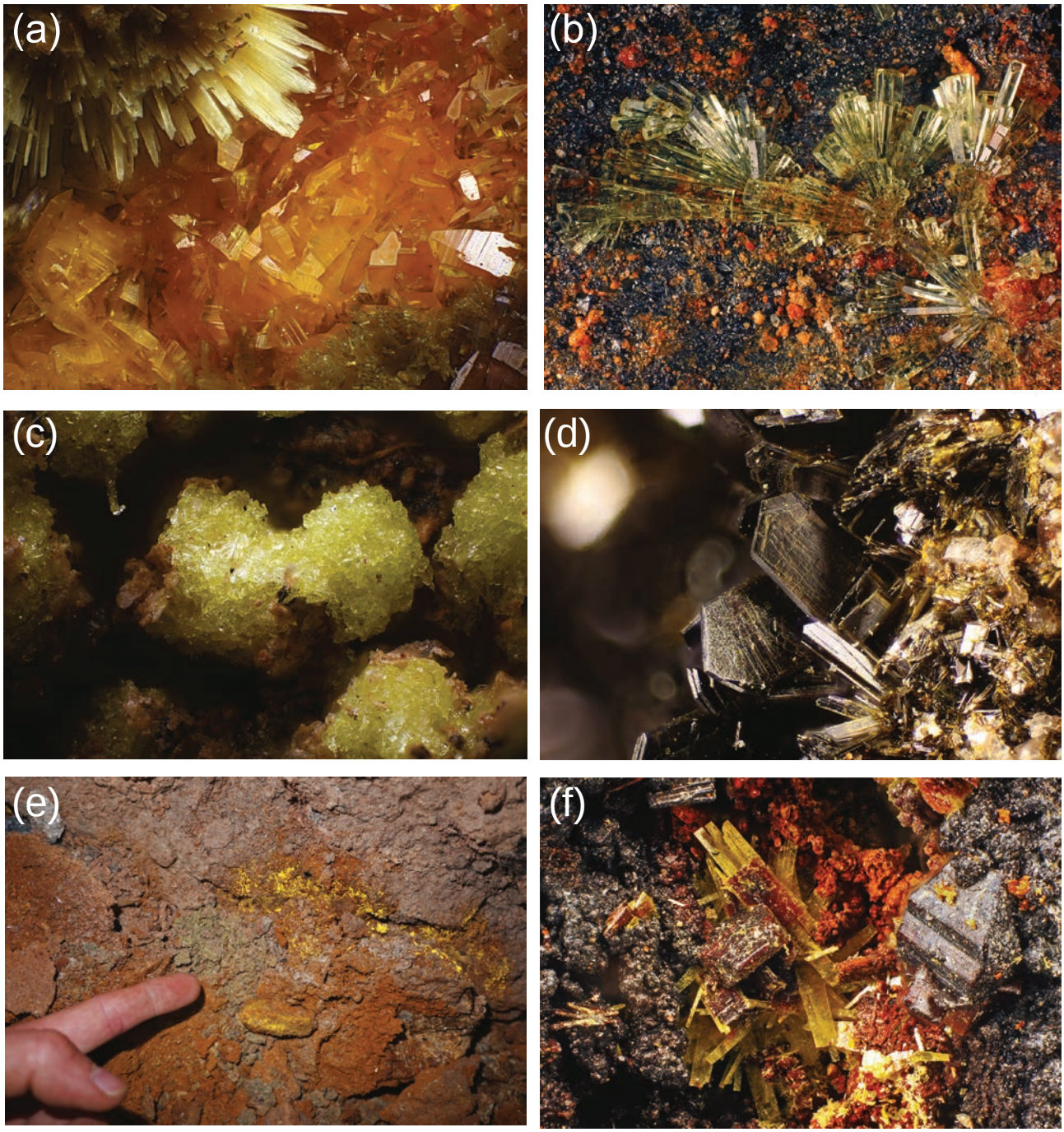

Fig. 7 Supergene uranium minerals. **a –** Uranyl carbonate rutherfordine (acicular) growing on silicate soddyite (short prismatic orange) from the Shinkolobwe mine, Congo. FOV 2.3 mm. **b –** Long-prismatic crystals of uranyl carbonate grimselite from Jáchymov. FOV 3.8 mm. **c –** Blocky aggregates of uranyl carbonate mineral bayleite from Jáchymov. FOV 2.5 mm. **d –** A rare uranyl carbonate mineral wyartite, containing U^{5+}. Shinkolobwe mine, Congo. FOV 2 mm. **e –** Typical efflorescence (uranyl sulphate marécottite) formed during acid mining drainage of uranium in a consolidated material on the floor of the mining adit. Jáchymov. **f –** Uranyl phosphate mineral phosphuranylite (yellow prismatic crystals) in the typical paragenesis of Fe-oxide–hydroxides forming pseudomorphs after older uranyl phosphate minerals – note the typical bipyramidal crystal of torbernite. Jáchymov. FOV 3.4 mm. All photos by P. Škácha, except for **e** (J. Plášil).

4. The change in pH conditions occurs usually when the vein sulfide minerals are completely leached out. The characteristic representatives are minerals of the phosphuranylite group, e.g. phosphuranylite (Fig. 7f), hügellite or dumontite. Such conditions also might occur far from the primary source (and sulfides) when U is remobilized. The buffer agents are then the surrounding rocks, i.e. lithological factors.

5. The last stage in the respective scheme (Fig. 6) is characteristic of alkaline or neutral conditions and involves the U^{4+}-bearing minerals, as reduced backwardly from UO_2^{2+}, *in situ* in the supergene zone. Typically, in such association occur secondary uraninite, coffinite, ningyoite and U^{4+} phosphates, such as poorly defined vyacheslavite, $U^{4+}(PO_4)(OH)\cdot nH_2O$ (Belova et al. 1984). However, it should be noted that not all U^{4+}-containing minerals should form under alkaline reducing conditions. For instance, recently documented unique association of secondary U^{4+}-bearing arsenate and sulfate minerals, štěpite, $U(AsO_3OH)_2(H_2O)_4$ (Plášil et al. 2013a) or běhounekite, $U(SO_4)_2(H_2O)_4$ (Plášil et al. 2011), formed from extremely acid solutions (pH ~0) derived from As-rich AMD at the Geschieber vein in Jáchymov.

Besides these general trends during uraninite weathering, it should be noted that the particular evolutionary path of the given mineral weathering association depends on the very local characteristics. These include the regional tectonics at the first place, geochemistry of the host-rocks, composition of primary ore and finally, the compositional evolution of the percolating ground water. Not unusual is also a cyclic character of the alteration with alternating occurrence (dominance) of e.g., uranyl phosphates and silicates, forming pseudomorphs or growing over one another. A nice contribution to the knowledge of the mechanisms of weathering of uranium deposits was published recently by Göb et al. (2013). Their study was focused on the remobilization of U and *REE* in the supergene zones of the Menzenschwand U-deposit in Schwarzwald (Black Forest Mts.), southwestern Germany, using ICP-MS analysis of the primary and supergene minerals, water geochemistry and geochemical modelling. The conclusions of this case study are probably of general validity, as shown by examples from various other uranium deposits. The sources for the *REE* in the system can be either uraninite and fluorite (like in some of the deposits in Black Forest Mts.) or the surrounding rocks. Based on the systematic study of PAAS-normalized *REE* patterns (Post-Archean Australian Sedimentary rocks), Göb et al. (2013) concluded that uranyl silicates formed under more reducing conditions (and lower pH) than uranyl phosphates and arsenates, documented with the lack of Ce^{3+} anomalies in studied uranyl silicates. The *REE* patterns of uranyl phosphates and arsenates studied resemble those of the mine-water samples, suggesting a uranium and *REE* transport from the source before crystallization. On the other hand, the *REE* patterns of uranyl silicates are similar to those of hydrothermal uraninites, suggesting the close origin of the supergene uranyl silicates and the primary ore (restricted redistribution and fractionation due to long-scale migration). The key-role for the pH–Eh changes plays the vein sulfide – its oxidation leads to the consumption of O_2 (thus the decrease of p_{O2}), drop in pH (due to increase in acid H^+) and increase of Fe^{3+} in the system. The transport or migration of *REE* is connected with mobile fluorine complexes. Thus there is a need for a source of F in order to maintain its high concentrations. In the case of Menzenschwand deposit (Göb et al. 2013), the likely source of *REE* was fluorite and the release of *REE* led to the crystallization of *REE*-phosphates (e.g. churchite-Y) at the late stages of the weathering. The precipitation of *REE*-phosphates, relatively younger than U-phosphates, is documented from various Variscan hydrothermal vein deposits. Illustrative examples represent Jáchymov (Ondruš et al. 1997) or Medvědín (Plášil et al. 2009) deposits in Bohemian Massif.

The role of radiogenic Pb during the alteration of uraninite is thought to be significant, at least for the decomposition of uraninite structure, as was documented by Janeczek and Ewing (1995), since Pb^{2+} is incompatible with fluorite-type structure at concentrations greater than a few percent. If the sulfur activity is high enough, galena (PbS) will form, and the volume of uraninite may change without any U^{6+} being released into the solution (Finch and Murakami 1999). If selenium activity is similarly high, clausthalite (PbSe) and other selenide minerals will form, as is well documented from the Variscan hydrothermal vein U-deposits. The same authors stated that, in the absence of sufficient sulfur in the system, uraninite may exsolve into Pb-rich and Pb-poor domains. In addition this may lead, along with auto-oxidation and hydration, to the formation of Pb–uranyl-oxide–hydroxy–hydrate minerals, as typically the early alteration products – vandendriesscheite, $[Pb_{1.6}(UO_2)_{10}O_6(OH)_{11}(H_2O)_{11}]$ and fourmarierite, $[Pb_{1-x}O_{3-2x}(UO_2)_4(OH)_4(H_2O)_{8x}]$. It is important to note that these processes are not isolated; it is not unusual that the specimen containing uraninite and remobilized younger sulfides or selenides, also contain Pb–uranyl-oxide–hydroxy–hydrate minerals. The process of Pb–U-mineral formation may be enhanced by preferential removal of U^{6+} as compared with Pb^{2+} at mineral surfaces by groundwaters. The reason is the high mobility of U^{6+} compared to Pb^{2+}, which results in the formation of Pb-rich minerals rinds in the residual masses ("*gummites*"). The Pb-rich uranyl-oxide–hydroxy–hydrates may form without high concentrations of dissolved Pb (Frondel 1958; Finch and Ewing 1992; Finch and Murakami 1999).

2.3. Thermodynamics of uranyl minerals

In order to assess, model and predict stabilities of uranyl minerals formed from primary phases during weathering, reliable thermodynamic data are necessary. In the past, these data were usually obtained from solubility experiments. A review of the solubility measurements for uranyl

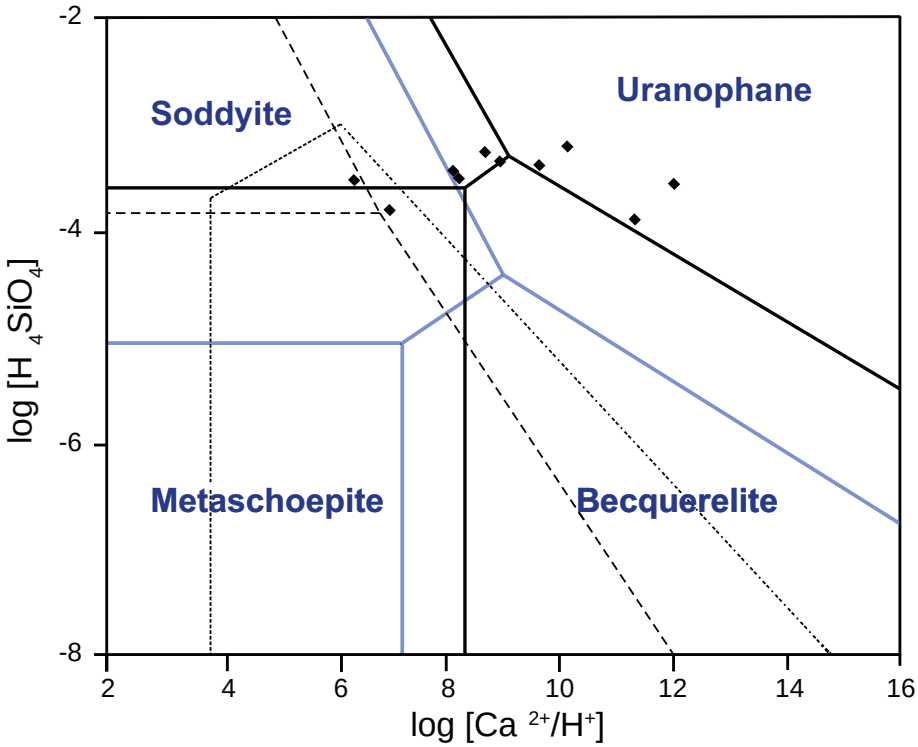

Fig. 8 Stability fields of minerals in the $CaO–SiO_2–UO_3–H_2O$ system based on experimental results (blue lines) and empirical model of Chen et al. (1999) (solid black lines). Stability fields derived by Finch and Ewing (1992) are shown by dashed lines with stability of becquerelite (dotted line) estimated from petrographic data. Black points are composition of groundwater and of J–13 water, respectively, taken from Chen et al. (1999). From Shvareva et al. (2012).

minerals was given by Gorman-Lewis et al. (2008a, b). Solubility experiments have been undertaken for only a limited number of uranyl minerals and compounds; however, the interesting empirical method developed by Chen et al. (1999) can be used to derive Gibbs free energies and enthalpies of formation. The method is based upon contribution of "isolated polyhedra" to the total Gibbs energy of the formation or enthalpy, respectively. During the past several years, new thermodynamic data for uranyl compounds obtained from solution calorimetry measurements have been presented (Kubatko et al. 2005, 2006; Gorman-Lewis et al. 2007, 2009; Shvareva et al. 2011, 2012; Navrotsky et al. 2013). A comparison of the thermodynamic values coming from solubility experiments, estimated using the method of Chen et al. (1999) and those from solution calorimetry was made by Shvareva et al. (2012) (Fig. 8). Importantly, the values obtained empirically, e.g., following the method developed by Chen et al. (1999), are only "rough" estimates when compared to more precise measurements. Still they remain useful in case such experiments cannot be done (Fig. 8).

3. Gaps, questions and future research

3.1. Mineralogy and crystallography

1. Mineralogical research on the new minerals, as the primary research goal, is (and should be) still on-going. Otherwise, after a certain time, there would not be anything "new" to study. Due to tremendous number of possible combinations of chemical constituents, occurring on Earth that can be accommodated in extremely complex structures of U-minerals, the number of the new uranium mineral species will undoubtedly increase.
2. The knowledge of the structural properties of U minerals is crucial for further assessment on the thermodynamic stability and other physical properties. Actually, there are still many U phases with unknown crystal structures. Uranyl minerals are usually hydrated oxysalts. There were done only few structure determinations for uranyl minerals/compounds with determined positions of the hydrogen atoms. This is namely due to the enormous difference in scattering power of uranium and hydrogen for the X-rays, used conventionally in the structural crystallography. The demand for the correct determination of the H_2O content and H positions arises from the fact that the role of H_2O in the structures of the hydrated oxysalts, particularly the uranyl minerals, is crucial (e.g., Hawthorne and Schindler 2008; Schindler and Hawthorne 2008; Hawthorne and Sokolova 2012; Hawthorne 2012).
3. Many U-containing minerals have unknown crystal structures (e.g., asselbornite, arsenovanmeerscheite, astrocyanite-(Ce), blatonite, heisenbergite, joliotite, paulscherrerite, uranospinite or voglite), and for many are available only qualitative refinements of their structures.

4. Several uranyl minerals have incorrectly determined crystal structures (e.g., phosphuranylite, Demartin et al. 1991) or should be discredited as the species completely (e.g., yingjiangite, Chen et al. 1990; Coutinho and Atencio 2000).

3.2. Weathering processes

1. In order to understand the key role of the processes taking place during weathering of uraninite, the most important is to decipher the sequence of such processes and redistribution of the elements (*REE*, U, Pb…) among primary and secondary minerals, either residual or newly precipitated, after transport in a solution.
2. Tracking the ages of various uranium mineralizations is vital in order to assess the sequence of the mineralization and alteration processes. In the past, many hypogene U-mineralizations were dated by the U–Pb method (e.g., Holliger 1991; Fayek et al. 2002; Evins et al. 2005; Sharpe and Fayek 2011). However, recently also supergene assemblages were dated using various techniques (Löfvendahl and Holm 1981; Maas et al. 2006; Neymark and Amelin 2008; Plášil et al. 2010b; Dill et al. 2010; Birch et al. 2011; Dill et al. 2011, 2013). Timing the supergene U-mineralizations is also important from another point of the view as it brings information about paleoclimatic conditions or changes (e.g., Dill et al. 2010).
3. Important for correct dating is the knowledge about redistribution of the radiogenic isotopes, especially radiogenic Pb, in the system. The prevalent opinion in the literature is that the majority of Pb incorporated in the newly formed Pb–uranyl-oxide minerals is radiogenic (e.g., Finch and Ewing 1992; Finch and Murakami 1999). The case study from the Variscan hydrothermal vein system at Březové Hory deposit in Příbram (Škácha et al. 2009) proved the necessity of the detailed research on the fate of both common and radiogenic Pb in hypogene and supergene U minerals.
4. It should be noted that the paragenetic scheme provided by Finch and Ewing (1992) with Finch and Murakami (1999) should be still considered as somewhat hypothetical, even if many paragenetic sequences observed in Nature suggest that these are indeed probable pathways. However, the classification of uraninites into “old” and “young” groups with regard to their Pb contents does not provide a fully functional scheme for understanding, as each uraninite contains some radiogenic Pb. The amount of the Pb in uraninite (and the possible lack of it) probably results from the different rates of alteration (e.g., variations in the rate of U remobilization).
5. Uranium is very sensitive to the redox conditions, and there is a large difference in mobility of reduced (U^{4+}) and oxidized (U^{6+}) species. Anyway, uranium occurs also as pentavalent (as e.g. mentioned mineral wyartite), namely when recurrently reduced from U^{6+} to U^{4+}. The role of U^{5+} in the crystalline phases, e.g. in uraninite itself, has not yet been documented and studied in detail.
6. The crystal structure of the self-irradiated natural uraninite should be investigated, since the methods used for studies of synthetic or natural materials designed for the long-term storage of nuclear waste (e.g., Lian et al. 2009; Zhang et al. 2010; Ewing 2011; Sureda et al. 2011; Deditius et al. 2012) have never been applied to the natural uraninite. This might help to improve our understanding of the kinetics of the uraninite alteration.
7. Detailed studies on the trace-element distribution, as for example provided by Göb et al. (2013), combined with the information about the age of the individual mineralization stages, are capable of revealing a more complete story about the evolution of such weathering associations.

3.3. Thermodynamics

1. Even though thermodynamic properties of several uraninite alteration products including uranyl–silicate (e.g., uranophane) or uranyl–oxide minerals, were determined recently, properties of many environmentally important phases, such as uranyl–sulfates, vanadates and some phosphates and arsenates, remain unknown or only poorly defined.
2. The verification of the known thermodynamic data for uranyl minerals needs to be done, e.g. with the same methodology used in recent studies but with different standards. Such verifications and cross-checks are very important, since the thermodynamic data may be used not only for explanation of geological processes in the past (e.g., genesis of the certain uranium deposit) but also of those currently taking place on Earth (e.g., contamination after the U-ore milling and the subsequent remediation).

Acknowledgements. First of all I would like to thank Jiří Čejka for his kindness and willingness he is helping the young scientists. Furthermore, I would like to acknowledge all the mentors and collaborators with whom I was able to collaborate since my early studies in Mineralogy as the bachelor student at the Faculty of Science of the Charles University in Prague. I am grateful to Alex Navrotsky, Sergey Krivovichev and Rob Raeside, who granted the permission to reprint figures from their original papers and also to Anatoly V. Kasatkin who provided a sample from his personal collection for the research. Pavel Škácha is acknowledged for the high-quality im-

ages of the uranium minerals. This paper benefited from the constructive reviews by Rod Ewing and Nicolas Meisser that helped significantly to improve its quality. Editorial handling by Jiří Sejkora and editor-in-chief Vojtěch Janoušek are highly appreciated. This work was financially supported by the post-doctoral grant of the GAČR no. 13-31276P.

References

Belova LN (1975) Oxidation Zones of Hydrothermal Uranium Deposits. Moscow, Nedra, pp 1–158 (in Russian)

Belova LN (2000) Formation conditions of oxidation zones of uranium deposits and uranium mineral accumulations in the gipergenesis (sic) zone. Geol Ore Dep 42: 103–110

Belova LN, Gorshkov AI, Ivanova OA, Sivtsov AV, Lizorkina LI, Voronikhin VA (1984) Vyacheslavite $U^{4+}(PO_4)(OH)\cdot nH_2O$ – a new uranium phosphate. Zap Vsesoyuz Mineral Obsh 113: 360–365

Birch WD, Mills SJ, Maas R, Hellstrom JC (2011) A chronology for Late Quaternary weathering in the Murray Basin, southeastern Australia: evidence from ^{230}Th/U dating of secondary uranium phosphates in the Lake Boga and Wycheproof granites, Victoria. Austr J Earth Sci 58: 835–845

Brown ID (1981) The bond-valence method: an empirical approach to chemical structure and bonding. In: O'Keeffe M, Navrotsky A (eds) Structure and Bonding in Crystals, vol. 2. Academic Press, New York, pp 1–30

Brown ID (2002) The Chemical Bond in Inorganic Chemistry. The Bond Valence Model. Oxford University Press, Oxford, pp 1–270

Brown ID (2009) Recent developments in the methods of the bond valence model. Chem Rev 109: 6858–6919

Brugger J, Meisser N, Burns PC (2003) Contribution to the mineralogy of acid drainage of uranium minerals: marecottite and the zippeite-group. Amer Miner 88: 676–685

Brugger J, Krivovichev SV, Berlepsh P, Meisser N, Ansermet S, Armbruster T (2004) Spriggite, $Pb_3[(UO_2)_6O_8(OH)_2](H_2O)_3$, a new mineral with α-$U_3O_8$-type sheets: description and crystal structure. Amer Miner 89: 339–347

Brugger J, Meisser N, Etschmann B, Ansermet S, Pring A (2011) Paulscherrerite from the Number 2 Workings, Mount Painter Inlier, Northern Flinders Ranges, South Australia: "dehydrated schoepite" is a mineral after all. Amer Miner 296: 229–240

Burns PC (1997) A new uranyl oxide hydrate sheet in vandendriesscheite: implications for mineral paragenesis and the corrosion of spent nuclear fuel. Amer Miner 82: 1176–1186

Burns PC (1998a) CCD area detectors of X-ray applied to the analysis of mineral structures. Canad Mineral 36: 847–853

Burns PC (1998b) The structure of richetite, a rare lead uranyl oxide hydrate. Canad Mineral 36: 187–199

Burns PC (1998c) The structure of compreignacite, $K_2(UO_2)_3O_2(OH)_3]_2(H_2O)_7$. Canad Mineral 36: 1061–1067

Burns PC (1999a) Cs boltwoodite obtained by the ion exchange from single crystals: implication for the radionuclide release in nuclear repository. J Nucl Mater 265: 218–223

Burns PC (1999b) The crystal chemistry of uranium. In: Burns PC, Ewing RC (eds) Uranium: Mineralogy, Geochemistry and the Environment. Mineralogical Society of America and Geochemical Society Reviews in Mineralogy and Geochemistry 38: 23–90

Burns PC (1999c) A new complex sheet of uranyl polyhedra in the structure of wölsendorfite. Amer Miner 84: 1661–1673

Burns P C (2005) U^{6+} minerals and inorganic compounds: insights into an expanded structural hierarchy of crystal structures. Canad Mineral 43: 1839–1894

Burns PC (2007) Crystal chemistry of uranium oxocompounds: an overview. In: Krivovichev SV, Burns PC, Tananaev IG (eds) Structural Chemistry of Inorganic Actinide Compounds. Elsevier, Amsterdam, pp 1–30

Burns PC, Finch RJ (1999) Wyartite: crystallographic evidence for the first pentavalent-uranium mineral. Amer Miner 84: 1456–1460

Burns PC, Hanchar J (1999) The structure of masuyite, $Pb[(UO_2)_3O_8(OH)_2](H_2O)_3$, and its relationship to protasite. Canad Mineral 37: 1483–1491

Burns PC, Hill F (2000) Implications of the synthesis and structure of the Sr analogue of curite. Canad Mineral 38: 175–181

Burns PC, Li Y (2002) The structures of becquerelite and Sr-exchanged becquerelite. Amer Miner 87: 550–557

Burns PC, Miller ML, Ewing RC (1996) U^{6+} minerals and inorganic phases: a comparison and hierarchy of crystal structures. Canad Mineral 34: 845–880

Burns PC, Ewing RC, Hawthorne FC (1997a) The crystal chemistry of hexavalent uranium: polyhedron geometries, bond-valence parameters, and polymerization of polyhedra. Canad Mineral 35: 1551–1570

Burns PC, Ewing RC, Miller ML (1997b) Incorporation mechanisms of actinide elements into the structures of U^{6+} phases formed during the oxidation of spent nuclear fuel. J Nucl Mater 245: 1–9

Burns PC, Finch RJ, Hawthorne FC, Miller ML, Ewing RC (1997c) The crystal structure of ianthinite, $[U^{4+}{}_2(UO_2)_4O_6(OH)_4(H_2O)_4](H_2O)_5$: a possible phase for Pu^{4+} incorporation during the oxidation of spent nuclear fuel. J Nucl Mater 249: 199–206

Burns PC, Deely KM, Skanthakumar S (2004) Neptunium incorporation into uranyl compounds that form as alteration products of spent nuclear fuel: implications for geologic repository performance. Radiochim Acta 92: 151–159

Cahill CL, Burns PC (2000) The structure of agrinierite: a Sr-containing uranyl oxide hydrate mineral. Amer Miner 85: 1294–1297

Čejka J, Urbanec Z (1990) Secondary uranium minerals. Transactions of the Czechoslovak Academy of Sciences, Mathematics and Natural History Series 100: pp 1–93

Cesbron F, Brown WL, Bariand P, Geffroy J (1972) Rameauite and agrinierite, two new hydrated complex uranyl oxides from Margnac, France. Mineral Mag 38: 781–789

Chen F, Ewing RC, Clark SB (1999) The Gibbs free energies and enthalpies of formation of U^{6+} phases: an empirical method of prediction. Amer Miner 84: 650–684

Chen Z, Yuzhu H, Xiaofa G (1990) A new mineral – yingjiangite. Acta Mineral Sin 10: 102–105 (in Chinese with English abstract)

Coutinho JMV, Atencio D (2000) Phosphuranylite from Minas Gerais, Brazil and its identity with yingjiangite. In: 4th International Mineralogy in Museums Conference, December 4th–7th, 2000, Program and Abstracts. Mineralogical Society of Victoria, Melbourne, pp 35

Deditius AP, Utsunomyia S, Ewing RC (2007a) Alteration of UO_{2+x} under oxidizing conditions, Marshall Pass, Colorado, USA. J All Comp 444–445: 584–589

Deditius AP, Utsunomyia S, Ewing RC (2007b) Fate of trace elements during alteration of uraninite in a hydrothermal vein-type U-deposit from Marshall Pass, Colorado, USA. Geochim Cosmochim Acta 71: 4954–4972

Deditius AP, Utsunomyia S, Ewing RC (2008) The chemical stability of coffinite, $USiO_4 \cdot nH_2O$; $0 < n < 2$, associated with organic matter: a case study from Grants uranium region, New Mexico, USA. Chem Geol 251: 33–49

Deditius AP, Pointeau V, Zhang JM, Ewing RC (2012) Formation of nanoscale Th-coffinite. Amer Miner 97: 681–693

Demartin F, Diella V, Donzelli S, Gramaccioli CM, Pilati T (1991) The importance of accurate crystal structure determination of uranium minerals. I. Phosphuranylite $KCa(H_3O)_3(UO_2)_7(PO_4)_4O_4.8H_2O$. Acta Cryst B47: 439–446

Dill HG, Weber B, Gerdes A (2010) Constraining the physical–chemical conditions of Pleistocene cavernous weathering in Late Palaeozoic granites. Geomorph 121: 283–290

Dill HG, Gerdes A, Weber B (2011) Dating of Pleistocene uranyl phosphates in the supergene alteration zone of Late Variscan granites by Laser-Ablation-Inductive-Coupled-Plasma Mass Spectrometry with a review of U minerals of geochronological relevance to Quaternary geology. Chem Erde 71: 201–206

Dill HG, Hansen BT, Weber B (2013) U/Pb age and origin of supergene uranophane-beta from the Borborema Pegmatite Mineral Province, Brazil. J South Am Earth Sci 45: 160–165

Evins LZ, Jensen KA, Ewing RC (2005) Uraninite recrystallization and Pb loss in the Oklo and Bangombé natural fission reactors, Gabon. Geochim Cosmochim Acta 69: 1589–1606

Ewing RC (1993) The long-term performance of nuclear waste forms: natural materials – three case studies. Mater Res Soc Symp Proc 294: 559–568

Ewing RC (2011) Actinides and radiation effects: impact on the back-end of the nuclear fuel cycle. Mineral Mag 75: 2359–2377

Fayek M, Kyser TK, Riciputi LR (2002) U and Pb isotope analysis of uranium minerals by ion microprobe and the geochronology of the McArthur River and Sue Zone uranium deposits, Saskatchewan, Canada. Canad Mineral 40: 1553–1569

Finch RJ, Ewing RC (1992) The corrosion of uraninite under oxidizing conditions. J Nucl Mater 190: 133–156

Finch RJ, Murakami T (1999) Systematics and paragenesis of uranium minerals. In: Burns PC, Ewing RC (eds) Uranium: Mineralogy, Geochemistry and the Environment. Mineralogical Society of America and Geochemical Society Reviews in Mineralogy and Geochemistry 38: pp 91–179

Finch RJ, Cooper MA, Hawthorne FC, Ewing RC (1996) The crystal structure of schoepite, $[(UO_2)_8O_2(OH)_{12}](H_2O)_{12}$. Canad Mineral 34: 1071–1088

Finch RJ, Hawthorne FC, Ewing RC (1998) Structural relations among schoepite, metaschoepite and "dehydrated schoepite". Canad Mineral 36: 831–845

Finch RJ, Burns PC, Hawthorne FC, Ewing RC (2006) Refinement of the crystal structure of billietite $Ba[(UO_2)_6O_4(OH)_6](H_2O)_8$. Canad Mineral 44: 1197–1205

Forbes TZ, Horan P, Devine T, McInnis D, Burns PC (2011) Alteration of dehydrated schoepite and soddyite to studtite, $[(UO_2)(O_2)(H_2O)_2](H_2O)_2$. Amer Miner 96: 202–206

Frondel C (1956) The mineralogical composition of gummite. Amer Miner 41: 539–568

Frondel C (1958) Systematic mineralogy of uranium and thorium. US Geol Surv Bull 1064: 1–400

Göb S, Guhring JE, Bau M, Markl G (2013) Remobilization of U and REE and the formation of secondary minerals in oxidized U deposits. Amer Miner 98: 530–548

Gorman-Lewis D, Mazeina L, Fein JB, Szymanovski JES, Burns PC, Navrotsky A (2007) Thermodynamic properties of soddyite from solubility and calorimetry measurements. J Chem Thermodyn 39: 568–575

Gorman-Lewis D, Burns PC, Fein JB (2008a) Review of uranyl mineral solubility measurements. J Chem Thermodyn 40: 335–352

Gorman-Lewis D, Fein JB, Burns PC, Szymanovski JES (2008b) Converse, solubility measurements of the uranyl oxide hydrate phases metaschoepite, compreignacite, Na-compreignacite, becquerelite, and clarkeite. J Chem Thermodyn 40: 980–990

Gorman-Lewis D, Shvareva T, Kubatko KA, Burns PC, Wellman DM, McNamara B, Szymanovsky JES, Navrotsky A, Fein JB (2009) Thermodynamic properties of autunite, uranyl hydrogen phosphate, and uranyl orthophosphate from solubility and calorimetric measurements. Envir Sci Technol 43: 7416–7422

Hawthorne FC (1983) Graphical enumeration of polyhedral clusters. Acta Cryst A39: 724–736

Hawthorne FC (1994) Structural aspects of oxide and oxysalt crystals. Acta Cryst B50: 481–510

Hawthorne FC (2012) A bond-topological approach to theoretical mineralogy: crystal structure, chemical composition and chemical reactions. Phys Chem Miner 39: 841–874

Hawthorne FC, Schindler M (2008) Understanding the weakly bonded constituents in oxysalt minerals. Z Kristall 223: 41–68

Hawthorne FC, Sokolova E (2012) The role of H_2O in controlling bond topology: I. The $^{[6]}Mg(SO_4)(H_2O)_n$ (n = 0–11) structures. Z Kristall 227: 594–603

Hazen RM, Ewing RC, Sverjensky DA (2009) Evolution of uranium and thorium minerals. Amer Miner 94: 1293–1311

Holliger P (1991) SIMS isotope analysis of U and Pb in uranium oxides: Geological and nuclear applications. In: Benninghoven A, Jansen KTF, Tümpner J, Werner HW (eds) Secondary Ion Mass Spectrometry (SIMS VIII). J. Wiley & Sons, Chichester, pp 719–722

Isobe H, Murakami T, Ewing RC (1992) Alteration of uranium minerals in the Koongarra deposit, Australia: unweathered zone. J Nucl Mater 190: 174–187

Janeczek J, Ewing RC (1992) Structural formula of uraninite. J Nucl Mater 190: 128–132

Janeczek J, Ewing RC (1995) Mechanisms of lead release from uraninite in the natural fission reactors in Gabon. Geochim Cosmochim Acta 59: 1917–1931

Janeczek J, Ewing RC, Oversby VM, Werme LO (1996) Uraninite and UO_2 in spent nuclear fuel: a comparison. J Nucl Mater 238: 121–130

Kampf AR, Mills SJ, Housley RM, Marty J, Thorne B (2010) Lead–tellurium oxysalts from Otto Mountain near Baker, California: IV. Markcooperite, $Pb(UO_2)Te^{6+}O_6$, the first natural uranyl tellurate. Amer Miner 95: 1554–1559

Kampf AR, Plášil J, Kasatkin AV, Marty J (2013) Belakovskiite, IMA 2013–075. CNMNC Newsletter No. 18, December 2013, page 3252; Mineral Mag 77: 3249–3258

Klingensmith A, Burns PC (2007) Neptunium substitution in synthetic uranophane and soddyite. Amer Miner 92: 1946–1951

Klingensmith A, Deely KM, Kinman WS, Kelly V, Burns PC (2007) Neptunium incorporation in sodium-substituted metaschoepite. Amer Miner 92: 662–669

Klomínský J, Veselovský F, Malec J (2013) Recent minerals in the Bedřichov water supply tunnel in Jizera Mts. – an example of the uranium release from the Jizera granite. Zpr Geol Výzk za r 2012: 2014–2019 (in Czech with English abstract)

Krivovichev SV, Plášil J (2013) Mineralogy and crystallography of uranium. In: Burns PC, Sigmon GE (eds) Uranium: From Cradle to Grave. Mineralogical Association of Canada Short Courses 43: pp 15–119

Kubatko KA, Helean KB, Navrotsky A, Burns PC (2005) Thermodynamics of uranyl minerals: enthalpies of formation of rutherfordine, UO_2CO_3, andersonite, $Na_2CaUO_2(CO_3)_3(H_2O)_5$, and grimselite, $K_3NaUO_2(CO_3)_3H_2O$. Amer Miner 90: 1284–1290

Kubatko KAH, Helean K, Burns PC, Navrotsky A (2006) Thermodynamics of uranyl minerals: enthalpies of formation of uranyl oxide hydrates. Amer Miner 91: 658–666

Langmuir D (1978) Uranium solution–mineral equilibria at low temperatures with applications to sedimentary ore. Geochim Cosmochim Acta 42: 547–569

Li Y, Burns PC (2000a) Investigations of crystal-chemical variability in lead uranyl oxide hydrates. I. Curite. Canad Mineral 38: 727–735

Li Y, Burns PC (2000b) Investigations of crystal-chemical variability in lead uranyl oxide hydrates. II. Fourmarierite. Canad Mineral 38: 737–749

Li Y, Burns PC (2001) The structures of two sodium uranyl compounds relevant to nuclear waste disposal. J Nucl Mater 299: 219–226

Lian J, Zhang JM, Pointeau V, Zhang FX, Lang M, Lu FY, Poinssot C, Ewing RC (2009) Response of synthetic coffinite to energetic ion beam irradiation. J Nucl Mater 393: 481–486

Löfvendahl R, Holm E (1981) Radioactive disequilibria and apparent ages of secondary uranium minerals in Sweden. Lithos 14: 189–201

Maas R, Mills S, Birch W, Hellstrom J (2006) U-series dating of secondary U phosphates – potential for improving chronologies of Late Pleistocene pluvial. ASEG Extended Abstracts 2006, 18th Geophysical Conference, pp 1–3

Meisser N, Brugger J, Ansermet S, Thélin P, Bussy S (2010) Françoisite-(Ce), a new mineral species from La Creusaz uranium deposit (Valais, Switzerland) and from Radium Ridge (Flinders Ranges, South Australia): description and genesis. Amer Miner 95: 1527–1532

Mereiter K (1986) Crystal structure and crystallographic properties of schröckingerite from Joachimsthal. Tschermaks Mineral Petrogr Mitt 35: 1–18

Mills SJ, Birch WD, Kolitsch U, Mumme WG, Grey IE (2008) Lakebogaite, $CaNaFe^{3+}{}_2H(UO_2)_2(PO_4)_4(OH)_2$

$(H_2O)_8$, a new uranyl phosphate with a unique crystal structure from Victoria, Australia. Amer Miner 93: 691–697

Murakami T, Ohnuki T, Isobe H, Sato T (1997) Uranium mobility during weathering. Amer Miner 82: 888–899

Navrotsky A, Shvareva T, Guo X (2013) Thermodynamics of uranium minerals and related materials. In: Burns PC, Sigmon GE (eds) Uranium: From Cradle to Grave. Mineralogical Association of Canada Short Courses 43: pp 147–164

Neymark LA, Amelin YV (2008) Natural radionuclide mobility and its influence on U–Th–Pb dating of secondary minerals from the unsaturated zone at Yucca Mountain, Nevada. Geochim Cosmochim Acta 72: 2067–2089

Ondruš P, Veselovský F, Hloušek J, Skála R, Vavřín I, Frýda J, Čejka J, Gabašová A (1997) Secondary minerals of the Jáchymov (Joachimsthal) ore district. J Czech Geol Soc 42: 3–76

Pagoaga MK, Appleman DE, Stewart JM (1987) Crystal structures and crystal chemistry of the uranyl oxide hydrates becquerelite, billietite, and protasite. Amer Miner 72: 1230–1238

Pearcy EC, Prikryl JD, Murphy WM, Leslie BW (1994) alteration of uraninite from the Nopal-I deposit, Peña-Blanca district, Chihuahua, Mexico, compared to degradation of spent nuclear-fuel in the proposed United-States high-level nuclear waste repository at Yucca Mountain, Nevada. Appl Geochem 9: 713–732

Pekov IV, Levitskiy VV, Krivovichev SV, Zolotarev AA, Bryzgalov IA, Zadov AE, Chukanov NV (2012a) New nickel–uranium–arsenic mineral species from the oxidation zone of the Belorechenskoye deposit, northern Caucasus, Russia: I. Rauchite, $Ni(UO_2)_2(AsO_4)_2.10H_2O$, a member of the autunite group. Eur J Mineral 24: 913–922

Pekov IV, Levitskiy VV, Krivovichev SV, Zolotarev AA, Chukanov NV, Bryzgalov IA, Zadov AE (2012b) New nickel–uranium–arsenic mineral species from the oxidation zone of the Belorechenskoye deposit, northern Caucasus, Russia: II. Dymkovite, $Ni(UO_2)_2(As^{3+}O_3)_2 \cdot 7H_2O$, a seelite-related arsenite. Eur J Mineral 24: 923–930

Pekov IV, Krivovichev SV, Yapaskurt VO, Chukanov NV, Belakovskiy DI (2013) Beshtauite, IMA 2012-051. CNMNC Newsletter No. 15, February 2013, page 3; Mineral Mag 77: 1–12

Piret P, Deliens M, Piret-Meunier J, Germain G (1983) La sayrite, $Pb_2[(UO_2)_5O_6(OH)_2] \cdot 4H_2O$, nouveau minéral; propriétés et structure cristalline. Bull Minéral 106: 299–304

Plášil J, Sejkora J, Ondruš P, Veselovský F, Beran P, Goliáš V (2006) Supergene minerals in the Horní Slavkov uranium ore district, Czech Republic. J Czech Geol Soc 51: 149–158

Plášil J, Sejkora J, Čejka J, Škoda R, Goliáš V (2009) Supergene mineralization of the Medvědín uranium deposit, Krkonoše Mountains, Czech Republic. J Geosci 54: 15–56

Plášil J, Sejkora J, Čejka J, Novák M, Viñals J, Ondruš P, Veselovský F, Škácha P, Jehlička J, Goliáš V, Hloušek J (2010a): Metarauchite, $Ni(UO_2)_2(AsO_4)_2 \cdot 8H_2O$, from Jáchymov, Czech Republic, and Schneeberg, Germany: a new member of the autunite group. Canad Mineral 48: 335–350

Plášil J, Čejka J, Sejkora J, Škácha P, Goliáš V, Jarka P, Laufek F, Jehlička J, Němec I, Strnad L (2010b) Widenmannite, a rare uranyl lead carbonate: occurrence, formation and characterization. Mineral Mag 74: 97–110

Plášil J, Dušek M, Novák M, Čejka J, Císařová I, Škoda R (2011a) Sejkoraite-(Y), a new member of the zippeite group containing trivalent cations from Jáchymov (St. Joachimsthal), Czech Republic: description and crystal structure refinement. Amer Miner 96: 983–991

Plášil J, Fejfarová K, Novák M, Dušek M, Škoda R, Hloušek J, Čejka J, Majzlan J, Sejkora J, Machovič V, Talla D (2011b) Běhounekite,$U(SO_4)_2(H_2O)_4$, from Jáchymov (St Joachimsthal), Czech Republic: the first natural U^{4+} sulphate. Mineral Mag 75: 2739–2753

Plášil J, Fejfarová K, Wallwork KS, Dušek M, Škoda R, Sejkora J, Čejka J, Veselovský F, Hloušek J, Meisser N, Brugger J (2012a) Crystal structure of pseudojohannite, with a revised formula, $Cu_3(OH)_2[(UO_2)_4O_4(SO_4)_2](H_2O)_{12}$. Amer Miner 97: 1796–1803

Plášil J, Hloušek J, Veselovský F, Fejfarová K, Dušek M, Škoda R, Novák M, Čejka J, Sejkora J, Ondruš P (2012b) Adolfpateraite, $K(UO_2)(SO_4)(OH)(H_2O)$, a new uranyl sulphate mineral from Jáchymov, Czech Republic. Amer Miner 97: 447–454

Plášil J, Hauser J, Petříček V, Meisser N, Mills SJ, Škoda R, Fejfarová K, Čejka J, Sejkora J, Hloušek J, Johannet J-M, Machovič V, Lapčák L (2012c) Crystal structure and formula revision of deliensite, $Fe[(UO_2)_2(SO_4)_2(OH)_2](H_2O)_7$. Mineral Mag 76: 2837–2860

Plášil J, Fejfarová K, Hloušek J, Škoda R, Novák M, Sejkora J, Čejka J, Dušek M, Veselovský F, Ondruš P, Majzlan J, Mrázek Z (2013a) Štěpite, $U(AsO_3OH)_2.4H_2O$, from Jáchymov, Czech Republic: the first natural arsenate of tetravalent uranium. Mineral Mag 77: 137–152

Plášil J, Kasatkin AV, Škoda R, Novák M, Kallistová A, Dušek M, Skála R, Fejfarová K, Čejka J, Meisser N, Goethals H, Machovič V, Lapčák L (2013b) Leydetite, $Fe(UO_2)(SO_4)_2(H_2O)_{11}$, a new uranyl sulfate mineral from Mas d'Alary, Lodève, France. Mineral Mag 77: 429–441

Plášil J, Kampf AR, Kasatkin AV, Marty J, Škoda R, Silva S, Čejka J (2013c) Meisserite, $Na_5(UO_2)(SO_4)_3(SO_3OH)(H_2O)$, a new uranyl sulfate mineral from the Blue Lizard mine, San Juan County, Utah, USA. Mineral Mag 77: 2975–2988

Schindler M, Hawthorne FC (2001) A bond-valence approach to the structure, chemistry and paragenesis of

hydroxyl–hydrated oxysalt minerals. II. Crystal structure and chemical composition of borate minerals. Canad Mineral 39: 1243–1256

Schindler M, Hawthorne FC (2004) A bond-valence approach to the uranyl-oxide hydroxy–hydrate minerals: chemical composition and occurrence. Canad Mineral 42: 1601–1627

Schindler M, Hawthorne FC (2008) The stereochemistry and chemical composition of interstitial complexes in uranyl–oxysalt minerals. Canad Mineral 46: 467–5017

Schindler M, Putnis A (2004) Crystal growth of schoepite on the (104) surface of calcite. Canad Mineral 42: 1667–1681

Schindler M, Mutter A, Hawthorne FC, Putnis A (2004a) Prediction of crystal morphology of complex uranyl-sheet minerals. I. Theory. Canad Mineral 42: 1629–1649

Schindler M, Mutter A, Hawthorne FC, Putnis A (2004b) Prediction of crystal morphology of complex uranyl-sheet minerals. II. Observations. Canad Mineral 42: 1651–1666

Schindler M, Hawthorne F C, Putnis C, Putnis A (2004c) Growth of uranyl–hydroxy–hydrate and uranyl–carbonate minerals on the (104) surface of calcite. Canad Mineral 42: 1683–1697

Schindler M, Hawthorne FC, Mandaliev P, Burns PC, Maurice PA (2011) An integrated study of uranyl mineral dissolution processes: etch pit formation, effects of cations in solution, and secondary precipitation. Radiochim Acta 99: 79–94

Sejkora J, Čejka J (2007) Šreinite from Horní Halže, the Krušné hory Mountains, Czech Republic, a new mineral species, its comparison with asselbornite from Schneeberg, and new data for asselbornite. Neu Jb Mineral, Abh 184: 197–206

Sharpe R, Fayek M (2011) The world's oldest observed primary uraninite. Canad Mineral 49: 1199–1210

Shvareva T, Mazeina L, Gorman-Lewis D, Burns PC, Szymanovski JES, Fein JB, Navrotsky A (2011) Thermodynamic characterization of boltwoodite and uranophane: enthalpy of formation and aqueous solubility. Geochim Cosmochim Acta 75: 5269–5282

Shvareva TY, Fein JB, Navrotsky A (2012) Thermodynamic properties of uranyl minerals: constraints from calorimetry and solubility measurements. Ind Eng Chem Res 51: 607–613

Škácha P, Goliáš V, Sejkora J, Plášil J, Strnad L, Škoda R, Ježek J (2009) Hydrothermal uranium–base metal mineralization of the Jánská vein, Březové Hory, Příbram, Czech Republic: lead isotopes and chemical dating of uraninite. J Geosci 54: 1–13

Sureda R, Casas I, Gimenez J, de Pablo J, Quinones J, Zhang J, Ewing RC (2011) Effects of ionizing radiation and temperature on uranyl silicates: soddyite $(UO_2)_2(SiO_4)(H_2O)_2$ and uranophane $Ca(UO_2)_2(SiO_3OH)_2.5H_2O$. Env Sci Technol 45: 2510–2515

Walenta K, Theye T (2012) Heisenbergite, a new uranium mineral from the uranium deposit of Menzenschwand in the Southern Black Forest, Germany. Neu Jb Mineral, Abh 189: 117–123

Walenta K, Hatért F, Theye T, Lissner F, Röller K (2009) Nielsbohrite, a new potassium uranyl arsenate from the uranium deposit of Menzenschwand, southern Black Forest, Germany. Eur J Mineral 21: 515–520

Weller MT, Light ME, Gelbricht T (2000) Structure of uranium(VI) oxide dihydrate, $UO_3 \cdot 2H_2O$; synthetic meta-schoepite $(UO_2)_4O(OH)_6 \cdot 5H_2O$. Acta Cryst B56: 577–583

Wronkiewicz DJ, Bates JK, Gerding TJ, Veleckis E (1992) Uranium release and secondary phase formation during unsaturated testing of UO_2 at 90 °C. J Nucl Mater 190: 107–127

Wronkiewicz DJ, Bates JK, Wolf SF, Bick EC (1996) Ten-year results from unsaturated drip tests with UO_2 at 90 °C: implications for the corrosion of spent nuclear fuel. J Nucl Mater 238: 78–95

Zhang JM, Livshits TS, Lizin AA, Hu QN, Ewing RC (2010) Irradiation of synthetic garnet by heavy ions and α-decay of ^{244}Cm. J Nucl Mater 307: 137–142